

**A.O.Maksimov**  
**OSCILLATION OF THE TETHERED BUBBLE**

Pacific Oceanological Institute, Far East Branch of Russian Academy of Sciences  
 43 Baltiyskaya ul., Vladivostok, 690041 Russia  
 Tel: (7-4232) 31 3081; Fax: (7-4232) 31 2573  
 E-mail: [maksimov@poi.dvo.ru](mailto:maksimov@poi.dvo.ru)

*The behaviour of a gas bubble tethered to a rigid plane boundary in an oscillatory pressure field is investigated by means of image theory. The inversion method is utilised to obtain an exact solution. This method is based on invariance of the Laplace equation to conformal transformations. The modified Rayleigh equation for the volume pulsation has been derived. It follows directly from this equation that the fundamental – the so-called ‘Minnaert’ frequency for the tethered bubble depends on the contact angle and this dependence is not monotonic.*

There are a number of acoustical techniques for bubble sizing. The effectiveness of these techniques is investigated in laboratory studies for simple controlled populations (stationary single tethered bubble) [1,2]. However, the influence of the boundary: wire [1], glass rod [2], or glass plate [3] on the bubble dynamics in an oscillating pressure field remains unclear. On the other hand, many attempts have been made by numerous researchers to study the interaction between a bubble and a rigid boundary [4-7]. In this study we present an analytical approach using image theory concerning the behaviour of a gas bubble near a rigid plane boundary, that gives a better physical insight into the dynamics of tethered bubbles.

Consider an air bubble of radius  $R_0$  driven by an acoustical wave of amplitude  $P_m$  and angular frequency  $\omega$ . As the radius of the bubble is often much smaller than the acoustic wavelength  $\lambda$  (i.e.  $R/\lambda = R\omega/c_0 \ll 1$ , where  $c_0$  is the sound speed in the liquid), there is effectively an ‘inner’ region around the bubble which may be regarded as incompressible. Thus the bubble dynamics may be modelled by considering the fluid to be inviscid and irrotational, leading to the velocity being expressed as  $\mathbf{v} = \nabla\phi$ ,  $\nabla^2\phi = 0$ .

The geometry of the problem is illustrated in Figure 1. The basic bubble equilibrium shapes show a segment of spherical profile, and the contact angle  $\vartheta_c$  is the angle obtained when this shape is extrapolated to the solid surface. The magnitude of  $\vartheta_c$  depends on wetting by the liquid of the material of the boundary and on the surface tension of the bubble wall. The diameter of the ring of contact is denoted by  $L$ . The relation between  $L$  and the equilibrium radius of the bubble  $R_0$  is given by  $L = 2R_0 \sin\vartheta_c$  and the volume of the spherical segment is

$$V_0 = (4\pi/3)R_0^3 \left[ 1 - (1/4)(1 - \cos\vartheta_c)^2 \right] (2 + \cos\vartheta_c)$$

The condition of no flow across the rigid boundary requires:  $(\partial\phi/\partial z) = 0$  on  $z = 0$ . The pressure in the liquid  $P$  is governed by the Bernoulli equation

$$P(\mathbf{r}, t) + \rho_0 \left[ \dot{\phi}(\mathbf{r}, t) + (\nabla\phi)^2 / 2 \right] = P_\infty + P_m \sin(\omega_p t) + \rho_0 \dot{\phi}_\infty(t) \tag{1}$$

where  $\rho_0$  and  $P_\infty$  are the equilibrium density and pressure, and  $P_m$  is the amplitude of the driving wave. The dynamic boundary condition is that the pressures on the two sides of the bubble wall differ only because of surface tension, i.e. if  $P_l$  and  $P_g$  denote the pressure in the water and in the bubble respectively, then

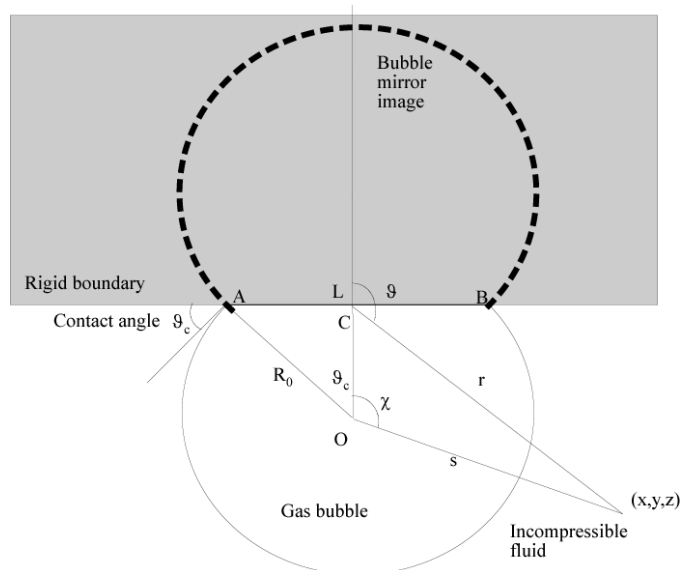


Figure 1.

$$P_l = P_g - (\sigma / \rho_0)(\nabla \cdot \mathbf{n}), \quad P_g = P_0 (V_0 / V)^\gamma \quad (2)$$

where  $\mathbf{n}$  is the unit vector normal to the bubble surface,  $\sigma$  is the coefficient of surface tension. We adopt a polytropic law for the gas in the bubble and  $V, V_0$  are the instantaneous and equilibrium bubble volume,  $\gamma$  is the polytropic exponent,  $P_0$  is the equilibrium pressure in the bubble. The kinematic boundary condition takes the form

$$\left[ \frac{\partial}{\partial t} + (\mathbf{v} \cdot \nabla) \right] (s - R)_{s=R_0+v} = 0, \quad s = \sqrt{x^2 + y^2 + (z + R_0 \cos \vartheta_c)^2} \quad (3)$$

The use of the image method to model the flow around a bubble near a rigid boundary has been first proposed by Cole [8], but we shall follow the approach derived by Kobelev & Ostrovskii [9]. As the pressure within the bubble is practically constant when  $R / \lambda \ll 1$  (homobaric bubble), its surface is equipotential if one neglects surface tension and the nonlinear inertial term in Bernoulli equation (1). We shall analyse only linear volume oscillations of relatively large bubbles  $R_0 \gg 1 \mu\text{m}$ , therefore can use this analogy with electrostatics. The velocity field  $\mathbf{v}$  in the liquid near the bubble wall will correspond to the electric field strength  $\mathbf{E}$  near the conducting body of the same shape. The normal component of the velocity on the bubble wall will be an analog of the surface charge density. The total charge  $Q$  will correspond to  $Q = \oint_S v_n dS = \dot{V}$ . The presence of the rigid boundary can be replaced by

the mirror image of the bubble relative to the plane  $z=0$  (see Figure 1) and thus the boundary condition of no flow will be automatically satisfied.

We derive an exact solution by use the inversion method [10]. This method is based on invariance of the Laplace equation to the definite class of transformation. It is easy to verify that this equation conserve its form under transformation  $r' = (l^2 / r)$  (inversion), if one transforms unknown function  $\varphi$  according to  $\varphi = (r' / l) \varphi'$ , here  $l$  is the radius of inversion. Thus if  $\varphi(\mathbf{r})$  is a solution of Laplace equation, than  $\varphi'(\mathbf{r}') = (l / r') \varphi[(l^2 / r'^2) \mathbf{r}']$  is also a solution.

Put the origin of the spherical system of coordinate in the point A (see Figure 1) and transform our problem with inversion radius equal to  $l = L = 2R_0 \sin \vartheta_c$ . The point B will be unchanged, the point A will go to point at infinity, and point at infinity will go to the origin of coordinates  $r' = (L^2 / r)$ , the bubble wall and the bubble wall mirror will transfer into a wedge with an angle equal to  $2\vartheta_c$ . Choosing the normalisation of  $\varphi$  such a way that its equipotential value vanishes on the bubble wall will lead to nonzero value of potential 'at infinity'  $\varphi_\infty$ . For the inverted potential it leads to the point source at the origin that redistribute charge density on the 'conducting' planes of the wedge where  $\varphi' = 0$ . The solution of this problem: point charge in conducting wedge is good known [10].

The potential  $\varphi'(r')$  is given by the formulae

$$\varphi' = \frac{Q}{2\vartheta_c \sqrt{2L\rho}} \int_\eta^\infty \frac{d\xi}{\sqrt{\cosh \xi - \cosh \eta}} \left[ \frac{\sinh\left(\frac{\pi\xi}{2\vartheta_c}\right)}{\cosh\left(\frac{\pi\xi}{2\vartheta_c}\right) - \cos\left(\frac{\pi(\theta - \vartheta_c)}{2\vartheta_c}\right)} - \frac{\sinh\left(\frac{\pi\xi}{2\vartheta_c}\right)}{\cosh\left(\frac{\pi\xi}{2\vartheta_c}\right) - \cos\left(\frac{\pi(\theta + \vartheta_c)}{2\vartheta_c}\right)} \right] \quad (4)$$

Here the cylindrical system of coordinates is used with the axis  $z'$  along the line of corner points, the angle  $\theta$  is counted off wedge plane,  $\cosh \eta = (L^2 + \rho^2 + z'^2) / (2L\rho)$ .

The auxiliary solution (4) provide the solution of our problem. Performing inverse transformation we obtain for Cartesian coordinate system with the origin at point C:

$$\varphi(x, y, z, t) = \frac{Q(t)}{2\sqrt{2}\vartheta_c \left[ (x^2 + y^2 + z^2 - L^2/4)^2 + z^2 L^2 \right]^{1/4}} \int_{\eta(x,y,z)}^\infty \frac{d\xi}{\sqrt{\cosh \xi - \cosh \eta(x, y, z)}} \times$$

$$\times \left[ \frac{\sinh\left(\frac{\pi\xi}{2\mathcal{G}_c}\right)}{\cosh\left(\frac{\pi\xi}{2\mathcal{G}_c}\right) - \cos\left\{\frac{\pi[\theta(x,y,z) - \mathcal{G}_c]}{2\mathcal{G}_c}\right\}} - \frac{\sinh\left(\frac{\pi\xi}{2\mathcal{G}_c}\right)}{\cosh\left(\frac{\pi\xi}{2\mathcal{G}_c}\right) - \cos\left\{\frac{\pi[\theta(x,y,z) + \mathcal{G}_c]}{2\mathcal{G}_c}\right\}} \right], \quad (5)$$

where  $\cosh \eta(x, y, z) = \left[ x^2 + y^2 + z^2 + (L^2/4) \right] \left[ \left[ x^2 + y^2 + z^2 - (L^2/4) \right]^2 + z^2 L^2 \right]^{-1/2}$ , and

$$\theta(x, y, z) = \mathcal{G}_c + \arccos \left\{ \left[ x^2 + y^2 + z^2 - (L^2/4) \right] \left[ \left[ x^2 + y^2 + z^2 - (L^2/4) \right]^2 + z^2 L^2 \right]^{-1/2} \right\}.$$

Far from the bubble  $r \gg L$  the potential is approached to  $\varphi(x, y, z, t) \xrightarrow{r \rightarrow \infty} (Q(t)/L) = Q(t)/(2R_0 \sin \mathcal{G}_c)$ , thus  $\dot{\varphi}_\infty$  contained in Bernoulli integral (1) is equal to  $\dot{\varphi}_\infty = \dot{Q}(t)/(2R_0 \sin \mathcal{G}_c)$ .

To find the displacement bubble wall we should substitute the solution (5) into the kinematic boundary condition (3). The normal derivation at the bubble wall has the simplest form in the spherical coordinate system with the origin coincided with the center of the bubble, when

$$\frac{\partial \varphi}{\partial n} = \frac{\partial \varphi}{\partial s} \Big|_{s=R_0} = \dot{v}(\kappa), \quad s = \sqrt{x^2 + y^2 + (z + R_0 \cos \mathcal{G}_c)^2}, \quad \cos(\kappa) = (z + R_0 \cos \mathcal{G}_c) / s.$$

By use the fact that  $\varphi|_{s=R_0} = 0$ , we obtain

$$\dot{v}(\kappa) = \frac{\partial \varphi}{\partial s} \Big|_{s=R_0} = \frac{Q(t)}{R_0^2} \frac{\pi}{4\sqrt{2}\mathcal{G}_c} \frac{\sin \mathcal{G}_c}{(\cos \mathcal{G}_c - \cos \kappa)^{3/2}} \int_{\cosh^{-1}\left(\frac{1 - \cos \mathcal{G}_c \cos \kappa}{\cos \mathcal{G}_c - \cos \kappa}\right)}^{\infty} \frac{d\xi}{\sqrt{\cosh \xi - \frac{1 - \cos \mathcal{G}_c \cos \kappa}{\cos \mathcal{G}_c - \cos \kappa}}} \frac{\sinh\left(\frac{\pi\xi}{2\mathcal{G}_c}\right)}{\cosh^2\left(\frac{\pi\xi}{2\mathcal{G}_c}\right)}. \quad (6)$$

This expression defines the way the normal displacement of bubble wall  $v$  depends on azimuthal angle  $\kappa$ . The volume of the bubble  $V$  and its time derivation are easily expressed through the normal displacement:

$$\dot{V} = 2\pi R_0^2 \int_{\mathcal{G}_c}^{\pi} \dot{v}(\kappa) \sin \kappa d\kappa. \quad (7)$$

Substituting the expression for normal displacement (6) into the equation (7) we obtain desirable result

$$\dot{V} = CQ, \quad \dot{\varphi}_\infty = [2R_0 \sin \mathcal{G}_c C(\mathcal{G}_c)]^{-1} \dot{V},$$

$$C(\mathcal{G}_c) = \frac{\pi^2}{2\sqrt{2}\mathcal{G}_c^2} \int_{\mathcal{G}_c}^{\pi} \frac{\sin \mathcal{G}_c \sin \kappa d\kappa}{(\cos \mathcal{G}_c - \cos \kappa)^{3/2}} \int_{\cosh^{-1}\left(\frac{1 - \cos \mathcal{G}_c \cos \kappa}{\cos \mathcal{G}_c - \cos \kappa}\right)}^{\infty} \frac{d\xi}{\sqrt{\cosh \xi - \frac{1 - \cos \mathcal{G}_c \cos \kappa}{\cos \mathcal{G}_c - \cos \kappa}}} \frac{\sinh\left(\frac{\pi\xi}{2\mathcal{G}_c}\right)}{\cosh^2\left(\frac{\pi\xi}{2\mathcal{G}_c}\right)} \quad (8)$$

Evaluating Bernoulli integral at bubble wall we get an analog of Rayleigh equation for the volume pulsation of tethered bubble

$$\frac{1}{2R_0 \sin \mathcal{G}_c C(\mathcal{G}_c)} \frac{d^2 V}{dt^2} + \frac{\gamma P_0}{\rho_0 V_0} \Delta V = -\frac{P_m}{\rho_0} \sin(\omega t). \quad (9)$$

It follows from this equation that the fundamental frequency of the tethered bubble has the form

$$\Omega_0^2(R_0, \mathcal{G}_c) = \Omega_0^{*2}(R_0) \sin \mathcal{G}_c C(\mathcal{G}_c) (2\pi)^{-1} \left[ 1 - (1/4)(1 - \cos \mathcal{G}_c)^2 (2 + \cos \mathcal{G}_c) \right]^{-1} \quad (10)$$

where  $\Omega_0^*(R_0) = \sqrt{3\gamma P_0 / \rho_0} R_0^{-1}$  is the fundamental frequency of a free bubble. The derived expression for the natural frequency (10) is given for the fixed radius of curvature  $R_0$  of spherical segment, but it is more interesting to trace how does the natural frequency of the bubble with the fixed volume  $V = (4\pi/3)R_0^3$  vary as it is tethered to the wall and the contact angle is changed?

$$\Omega_0^2(V, \vartheta_c) = \Omega_0^{*2}(V) \sin \vartheta_c C(\vartheta_c) (1/2) \left[ 1 - (1/4)(1 - \cos \vartheta_c)^2 (2 + \cos \vartheta_c) \right]^{-1/3}. \quad (11)$$

The Figure 2 illustrates the dependence of  $\Omega_0(V, \vartheta_c)/\Omega_0^*(V)$  on the contact angle  $\vartheta_c$ , here  $\Omega_0^*(V)$  is the natural frequency of the free bubble. This nonmonotonic relation is surprising at first glance, but can be explained the following way. As the oscillating gas bubble is approached to the rigid boundary its inertial mass is increased. Really as has been mentioned above the presence of rigid boundary is equivalent to the presence of the mirror bubble oscillating synchronous with the first one. Now it is more difficult for the bubble to accelerate the fluid in the region between its mirror, as the second (mirror) bubble acts with opposite force. As a result the inertial mass grows and the fundamental frequency decreases as the bubble is approached to the boundary. When the bubble touch the boundary ( $\vartheta_c = 0$ ), the area where the bubble and its mirror hinder each other to accelerate the fluid begin to shrink and as a result the inertial mass will decrease, the natural frequency begin to increase. This growth will continue till the limit of applicability our approach – homobaricity within the bubble that is till the wavelength will be compared with base of the spherical segment.

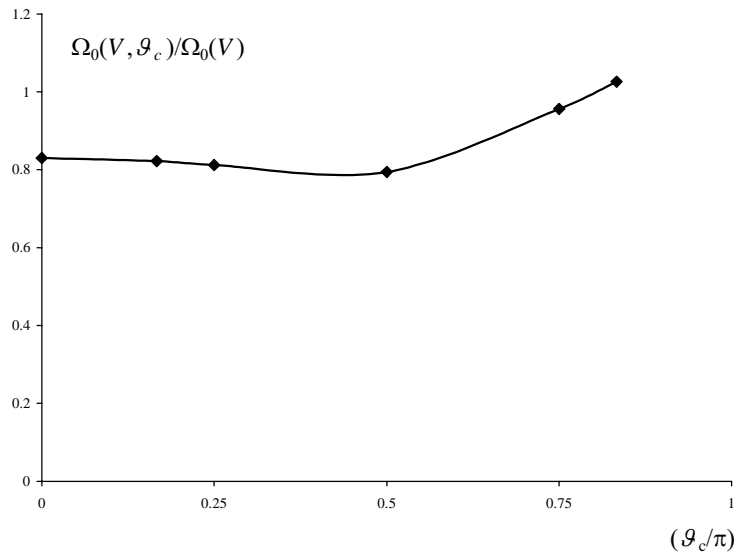


Figure 2.

When the bubble touch the boundary ( $\vartheta_c = 0$ ), the area where the bubble and its mirror hinder each other to accelerate the fluid begin to shrink and as a result the inertial mass will decrease, the natural frequency begin to increase. This growth will continue till the limit of applicability our approach – homobaricity within the bubble that is till the wavelength will be compared with base of the spherical segment.

This work has been supported by The Russian Foundation for Basic Research under grants numbers 01-05-64915 and 04-02-16412.

### REFERENCES

1. Leighton T.G., Phelps A.D., Ramble D.G., Sharpe D.A. Comparison of the abilities of eight acoustic techniques to detect and size a single bubble // Ultrasonics. 1996. V.34. P.661-667.
2. Birkin P.R., Watson Y.E., Leighton T.G. and Smith K.L Electrochemical detection of Faraday waves on the surface of a gas bubble. // Langmuir Surfaces and Colloids. 2002 V.18. P.2135-2140.
3. Hardwick A.J. The mechanism of subharmonic ultrasound modulation by forcibly oscillating bubbles. Ultrasonics. 1996. V.33. P.341-343.
4. Blake J.B., Taib B.B., Doherty G. Transient cavities near boundaries. Part 1. Rigid boundary. // J. Fluid Mech. 1986. V.170. P. 479-497.
5. Blake J.B., Gibson D.C. Cavitation bubbles near boundaries. // A. Rev. Fluid Mech. 1987 V.19. P.99-123.
6. Sato K., Tomita Y., Shima A. Numrical analysis of a gas bubble near a rigid boundary in an oscillating pressure field. // J. Acoust. Soc. Am. 1994 V.95. P.2416-2424.
7. Blake J.R., Keen G.S., Tong R.P., Wilson M. Acoustic cavitation: the fluid dynamics of non-spherical bubbles. // Phil. Trans. R. Soc. Lond. A 1999 V.357. P.251-267.
8. Cole R.H. Underwater explosions. Princeton: Princeton U.P., 1948.
9. Kobelev Yu.A., Ostrovskii L.A. Acousto-electrostatic analogy and gas bubbles interaction in liquid. // Sov. Phys. Acoust. 1984. V.30. P.715-716.
10. Landau L.D., Lifshitz E.M. Electrodynamics of continuos medium. Moscow: Nauka, 1982, 624 P. (in Russian)